Mapping the northern and southern extent of the Socorro midcrustal magma body by wide-angle seismic reflections

Kenneth H. Olsen, Dan J. Cash, and John N. Stewart
1982, pp. 179-185. https://doi.org/10.56577/FFC-33.179

in:

Albuquerque Country II, Wells, S. G.; Grambling, J. A.; Callender, J. F.; [eds.], New Mexico Geological Society 33 rd Annual Fall Field Conference Guidebook, 370 p. https://doi.org/10.56577/FFC-33

This page is intentionally left blank to maintain order of facing pages.

MAPPING THE NORTHERN AND EASTERN EXTENT OF THE SOCORRO MIDCRUSTAL MAGMA BODY BY WIDE-ANGLE SEISMIC REFLECTIONS

KENNETH H. OLSEN, DAN J. CASH, and JOHN N. STEWART
Earth and Space Sciences Division
University of California
Los Alamos National Laboratory
Los Alamos, New Mexico 87545

INTRODUCTION

This paper reviews seismological studies of a deep seated, but not readily apparent, volcano-tectonic structure beneath the Albuquerque basin. This is a midcrustal magma body (MCMB) whose existence has been inferred from various geophysical evidence. Although the details and mechanisms are presently obscure, this anomalous feature probably plays an important role in the evolution of the Rio Grande rift. Filling in these details is the aim of continuing research by many investigators. We concentrate here on inferred physical properties of the MCMB, based largely on our "wide-angle" seismic refraction profiling experiments, but also including reviews of microearthquake studies and vertical profiling work by others. Figure 1 is a schematic representation of the three methods. Data from each seismological method emphasize somewhat different aspects of the MCMB and need to be combined to form an integrated picture. Discussion of other kinds of geophysical evidence has been reviewed by Sanford and others (1977) and by Rinehart and others (1979).

NEW MEXICO TECH MICROEARTHQUAKE STUDIES

As early as 1965, Sanford and Long (1965) reported unusual seismic phases on recordings of shallow microearthquakes near Socorro, New Mexico. Continuing work by Sanford and colleagues (Sanford and others, 1973, 1977; Rinehart and others, 1979), using temporary arrays of portable seismographs in the vicinity of Socorro, established that these unusual features on the seismograms are caused by seismic energy strongly reflecting off a layer in the earth's crust about 18-20 km deep and arriving at the seismograph several seconds behind the seismic energy burst that travels a shorter, more direct path from the microearthquake to the recording station. Sanford and others' (1977) analysis of the character of these reflections further established they are mainly due to incident S-wave (shear wave) energy reflected back toward the surface as either S-waves or as P-waves converted from S at the reflector surface (these are known as S x S and S x P phases, respectively); P-wave reflection phases (P x P) from incident compressional (P-waves) are poorly observed. The interface material at 20 km depth displaying these particular reflecting properties is deduced to have a very small *in situ* shear wave velocity, i.e., it has the properties of a fluid. The comparatively large depth (20 km), high heat flow, and other geophysical evidence (Sanford and others, 1977) leads to the conclusion that magma or partially molten rock makes up the reflecting layer. The fraction of partial melt need only be a few percent to explain the observed S x S and S x P reflection amplitudes (Rinehart and others, 1979).

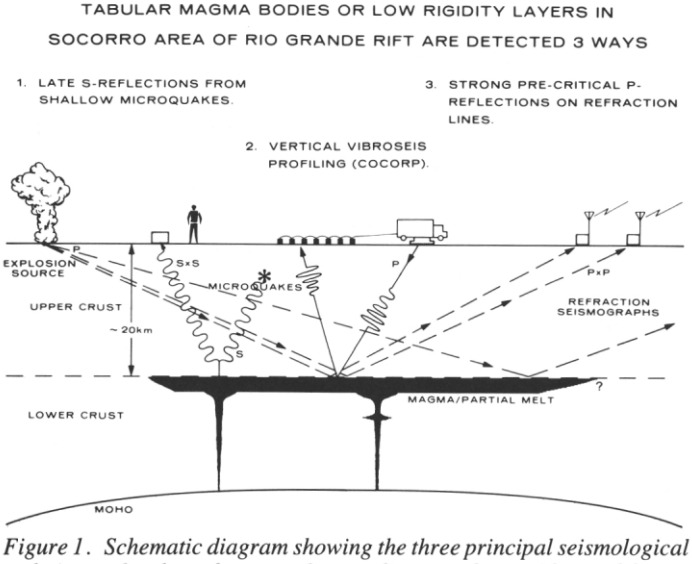

Figure 1. Schematic diagram showing the three principal seismological techniques that have been used to study anomalous midcrustal layers in the central Rio Grande rift.

These unusual reflecting properties of the inferred magma body enabled Rinehart and others (1979) to map the extent of this anomalous midcrustal layer over an area of 1,700 km= from Socorro northward into the Albuquerque-Belen basin of the Rio Grande rift. Source microearthquakes (a microearthquake is defined as an earthquake with a magnitude less than 3) used to map the magma body by this technique come mainly from layers that overlie the magma body (focal depths between 4 and 10 km). Indeed, these microearthquakes, which tend to occur in swarms, are probably caused by bulging of the overlying layers by injection and movement of magmatic fluid within the midcrustal layer itself. Thus, the presently mapped 1,700-km= lateral extent of the magma layer is partly determined by whether frequent shallow microearthquakes exist that provide S-wave energy that reflects from the underlying anomalous zone. Earthquakes in the Socorro "swarm area" are most numerous near the intersection of the Morenci and Capitan lineaments (Ward and others, 1981) about 15 km southwest of Socorro, so lateral edges of the midcrustal magma body are well determined there. Farther north toward Belen in the Albuquerque basin, microearthquake are fewer, so the magma body boundaries there are uncertain because of lack of sources. Other interesting properties of the MCMB deduced from microearthquake array studies are: (1) it is less than 1 km in thickness because steeply incident P-waves traveling upward through the crust from very distant seismic sources are not significantly delayed by the anomalous region (Rinehart and others, 1979), and (2) the upper reflector surface has very low relief over its entire extent and dips less than 6° northward, suggesting a fluid-like upper surface perhaps capped by an overlying barrier.

In addition to microearthquake studies outlined above and other types of geophysical evidence (heat flow, anomalous low crustal electrical resistivity, geodetic bulging, etc.), two other seismological techniques have been used to study the properties of the MCMB. These are in-

dicated pictorially in Figure 1. Each method provides information about the MCMB which both supplements and complements the microearthquake technique.

VERTICAL REFLECTION PROFILING

The vertical reflection profiling technique used by the Consortium for Continental Reflection Profiling (COCORP) is an adaptation and extension of a technique widely used by the oil industry to probe layered structures above crystalline basement. The COCORP operation uses several phase-linked, truck-mounted vibrators to transmit a frequency modulated ("chirp" or "sweep") seismic-wave packet into the ground (Oliver, 1978). Reflected energy from subsurface discontinuities is detected by a linear spread of closely spaced seismic sensors, and the signals are computer correlated with the unique source wavelet in order to reduce interfering noise and to enhance coherent echoes that indicate deep structures. The 1975-77 COCORP profiling in the Rio Grande rift differed from standard oil-industry procedure mainly in using greater input energy (five vibrators) and recording for longer durations (about 40-50 seconds) in order to accept any reflected energy from depths down to 50 km (Brown and others, 1979, 1980). It is important to note that current reflection profiling equipment and signal processing is primarily restricted to compressional wave (P-wave) sources and reflections traveling nearly vertically. Thus, structures and interfaces whose properties differ mainly in S-wave velocities rather than P-wave contrasts are not well delineated by vertical reflection profiling methods, so these need to be supplemented by additional techniques such as refraction. In addition, calculation of relief and depths of structures from echo-time measurements requires accurate velocity measurements that are better determined by wide-angle refraction measurements.

The 1975-77 COCORP lines pertinent to studies of the MCMB in the Rio Grande rift are shown as lines with numbered triangular end points in Figure 2. Abo Pass line 1 ran eastward from the Tertiary-Quaternary graben fill of the Albuquerque basin through Abo Pass to the Paleozoic formations on the eastern rift flank. Line 2 ran subparallel with the trend of the rift and crossed line 1 west of Abo Pass. Line IA extends from Abo Pass across the rift into Colorado Plateau structure near Sierra Lucero on the western flank of the rift. Lines 3 and 4 cross the seismically active area southwest of Socorro (fig. 2). Brown and others (1979, 1980) review many intra-rift, upper crustal reflectors delineated by these surveys; our discussion is limited to COCORP reflection data pertaining to the MCMB (Brocher, 1981) and to how these data can be combined with the microearthquake surveys and with our wide-angle refraction surveys to give information on the physical properties of the MCMB.

Brocher (1981) concluded that vertical COCORP reflection survey data (mainly along lines 1, 1-A, and 2) suggest a model of the MCMB with the following features.

1. Analysis of COCORP data on near vertical-incidence P x P reflections from the midcrustal level are best done from lines 1 and 2 (fig. 2) because of higher data quality and simpler near-surface structure. Poorer data quality on lines 1-A, 3, and 4 (fig. 2) prevent good midcrustal interpretation of these areas. "Edges" of the MCMB as determined from COCORP vertical P x P reflections near Highway 60 and near the Ladron Mountains are shown as stippled areas crossing profiles in Figure 2.

2. The COCORP input sweep signal varied smoothly between frequencies of 10 and 32 Hz. The P x P reflectivity (approximately the same as the reflection coefficient, see below) obtained from Brocher's (1981) data inversion calculations varies with frequency in a complex manner and is usually sharply peaked near 26 Hz.

3. Rapid lateral variations in the amplitudes of narrow angle P x P reflections along COCORP profiles, as well as strongly variable and peaked frequency dependence of the reflectivity, forcibly suggest that these are wave interference effects caused by a complex, thinly-laminated structure at the reflector depth.

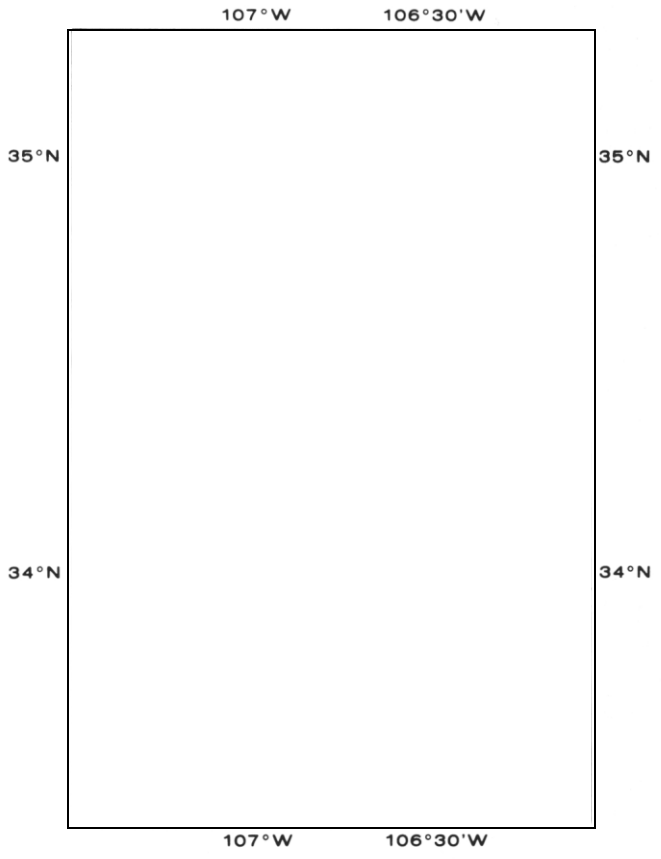

Figure 2. Map of central New Mexico between Albuquerque and San Marcial showing locations of seismic studies. The extent of the MCMB near Socorro is shown in stippled pattern with edges dashed where uncertain. Solid lines with triangular end markers indicate COCORP profiles. Refraction profiles from the DICE THROW and BUTTERFLY MAIDEN shotpoints (asterisks) are shown as dashed lines. Diagonal hatching indicates reflection point regions at midcrustal depths where strong P×P phases are observed; patterned circles are subsurface areas where no P×P phases can be detected.

4. To explain the above observations, Brocher (1981) proposes a model of the MCMB that consists of several low-velocity magma or partial-melt layers, each with thicknesses of 30-40 m, separated by country-rock layers of similar thickness (about 60 m) and of near normal upper-crustal compressional velocity (6 km/s). The MCMB in areas showing strong COCORP reflections is envisioned as a complex sill-like intrusive consisting of alternating thin (tens of meters) layers of high- and low-velocity material with various partial melt fractions. This intrusive model for the central rift parts of the MCMB is consistent with a picture of the physical nature of the midcrustal layer suggested by somewhat different seismic data from microearthquake studies and wide-angle refraction profiling.

CRUSTAL REFRACTION PROFILING

The seismic-refraction method is the third seismic technique depicted in Figure 1, and it forms the basis for most of our analysis. In crustal refraction profiling, impulsive sources (generally shallowly buried explosions) are detonated, and recording stations laid out along lines radial from the source at intervals of 1 to 5 km to distances of 100 to 200 km receive the impulses. Raypaths for seismic waves refracted and

reflected from discontinuities and velocity-gradient zones in the crust and mantle are incident on crustal layers at large angles (greater than 30° as measured from the vertical). One advantage of the refraction technique is the predominantly horizontal travel of seismic waves. Reliable average P-wave (and in some cases S-wave) velocities can then be derived as a function of depth. Seismic velocities are frequently the most reliable indicators of densities and petrological conditions available from levels beyond drilling depths. Interpretation of refraction profiles near the Rio Grande rift by Toppozada and Sanford (1976) and by Olsen and others (1979) established the main features of crustal structure down to the Moho, which is about 35 km deep beneath the central rift near Albuquerque. Refraction profiling also establishes: (1) that the crust is thinner (35 km) beneath the rift than beneath adjacent areas of the Great Plains (50 km) and Colorado Plateau (40 km); (2) that the compressional ("P_n") mantle velocity beneath the rift axis is anomalously low (7.6-7.8 km/s); and (3) that distinct upper crustal (V_p = 6 km/s) and lower crustal (V_p about 6.4 km/s) layers exist in this part of the rift. The boundary between the petrologically different upper and lower crustal layers occurs at the same depth (18 to 20 km) as the top of the MCMB, perhaps implying a relationship between deep intrusion mechanisms and evolution of the continental crust into two principal components.

We studied seismic waves generated by chemical explosion tests at White Sands Missile Range in 1976 (referred to as DICE THROW) and at Kirtland Air Force Base in 1981 (referred to as BUTTERFLY MAIDEN, or BFLY) to infer features of crustal structure along a 150-km-long profile between Albuquerque and the Oscuro Mountains (fig. 2). The lines along which portable seismic recorders were deployed (shown dashed in fig. 2) ran along the western foothills of the Manzano Mountains (eastern edge of Albuquerque basin), through Abo Pass, and along the eastern flanks of the Los Pinos range to the vicinity of Bingham. The south-to-north line from the 1976 DICE THROW shotpoint was part of the longer (350 km) refraction profile along the axis of the Rio Grande rift already interpreted by Olsen and others (1979) for crustal structure down to mantle depth; here, we are concerned only with depths to 30 km. The 1981 BFLY shot was considerably smaller than DICE THROW (16 tons and 600 tons, respectively) so adequate signals were obtained only for distances less than about 100 km from the source.

Figure 3 is a time-distance display of seismograms recorded out to 125 km from DICE THROW. Each seismogram in the record section has been time shifted by an amount depending on its distance form the source such that a signal traveling at an apparent velocity of 6.0 km/s appears as a horizontal line in the diagram (e.g., the P_g phase that propagates mainly along the top of the granitic basement travels at this average speed). Phases with apparent velocities greater than 6.0 km/s have negative slope; curvature of phase correlation lines such as P x P and PmP in Figure 3 are characteristic of reflections from nearly horizontal subsurface horizons ("moveout"). As discussed by Olsen and others (1979), the enhanced amplitudes closely following the PmP phase correlation curve of Figure 3 are "pre-critical distance" compressional-wave reflections from the Moho at 35-km depth. The seismological nomenclature for such P-wave-to-P-wave reflection at the Moho is PmP. An even more striking pre-critical reflection phase appearing on the DICE THROW section is what we call P x P (fig. 3) arising from a discontinuity ("layer X") at 20-km depth. Within experimental uncertainty, this 20-km depth is the same as that determined by the New Mexico Tech and COCORP investigators for the magma body in areas west of our profiles. Even though reflected and refracted phases from midcrustal layers are commonly seen on refraction profiles throughout the world, the DICE THROW P x P phases are highly unusual in that (1) they are very strong (in some seismograms, they are the largest amplitude feature), and (2) they can easily be traced back to stations as close as 40 km (and perhaps to 25 km) from the source. Most strong reflections on refraction profiles are "post-critical," grazing incidence phases only observable at distances beyond 100 km.

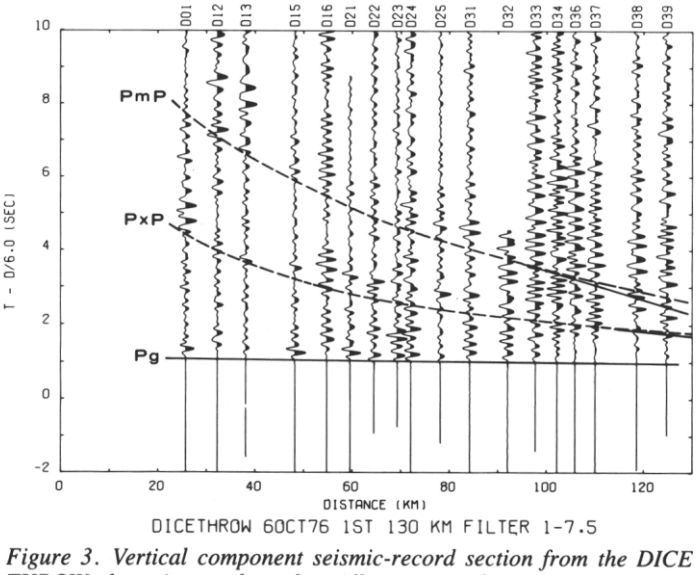

Figure 3. Vertical component seismic-record section from the DICE THROW shotpoint northward to Albuquerque showing superimposed travel-time curves for Pg, P×P, and PmP phases. Note particularly large amplitudes of P×P between 38 and 98 km.

As sketched in Figure 1, the point at which reflection occurs at the subsurface interface ("reflection point" or "turning point") lies approximately halfway between the source and the receiving seismograph. A line of seismographs ranging from 40 to 100 km, for example, defines reflection points between distances of 20 to 50 km. The 1981 north-to-south BFLY profile reversed the DICE THROW line and also shows prominent P x P arrivals over parts of its length. Figure 4 is a particularly clear example of strong, wide-angle P x P, following P_n arrivals by about 1.7 seconds as recorded by a radial tripartate array at a mean distance of 85 km from the shotpoint. The diagonally hatched areas of Figure 2 indicate reflection points along a 20-km-deep interface where strong P x P are observed. The area north of Abo Pass is the one covered best by BFLY observations; the area just north of Highway 380 (latitude 34°N) is the area of strong P x P reflection points seen in DICE THROW records. Dotted circles (see fig. 2) 7 to 30 km south of BFLY shotpoint indicate sub-surface reflection points where *no* P x P could be discerned.

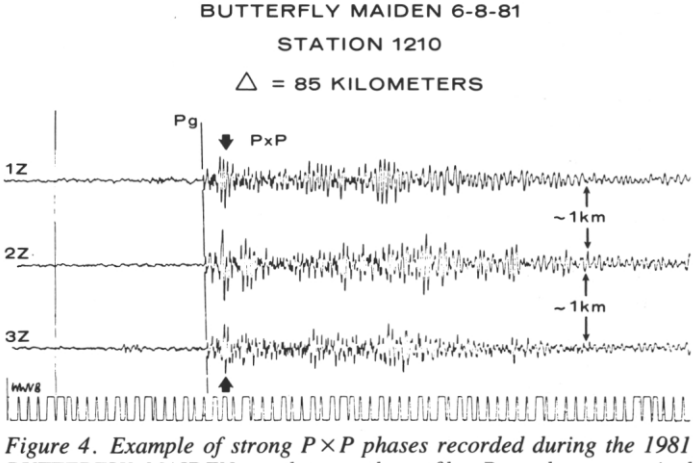

Figure 4. Example of strong P×P phases recorded during the 1981 BUTTERFLY MAIDEN north-to-south profile. Records are vertical component traces from matched seismometers separated by about 1 km along a line radial to the shot. Distance between each spike on the WWVB timing trace at the bottom represents 1 second.

The apparent 35-km "gap" in P x P reflection points south of Abo Pass may not indicate a lateral discontinuity in the midcrustal reflecting surface but instead a region where any P x P reflection from either shotpoint could overlap with PmP and 1[3], arrivals and be difficult to resolve with confidence. Wide-angle P x P for this section of the profiles would have to be observed on stations at 110-to-190-km ranges; Figure 3 indicates how all phases merge at these distances. Shotpoints at other locations are needed to establish the presence or absence of the midcrustal reflector outside the hatched areas of Figure 2 by this technique. Unshaded areas of Figure 2 are thus areas of "absence of evidence" rather than regions of "evidence of absence" in regard to the anomalous midcrustal reflector.

In addition to our profiles along the western edge of the Albuquerque basin, E. Rinehart and L. Jacksha (personal commun., 1981) used the same technique to make wide-angle "spot" measurements of P x P on the BFLY shot. They used portable recorders near the Ladron and the Magdalena mountains (points LJ and SC in Figure 2). LJ stations observed no P x P from a reflection point just north of Belen, and SC stations recorded extremely strong P x P from a reflection point near the junction of Highway 60E, Interstate 25, and COCORP line 1-A.

INTERPRETATION OF MCMB REFLECTIONS

The character of P x P, S x S, and S x P reflections obtained by the three different seismic methods give important clues about the physical nature of the MCMB. Interpretation of seismic refraction profiles has been greatly facilitated in recent years by the technique of synthetic seismogram modeling. Synthetic modeling makes use of large, fast computers to calculate amplitude calibrated waveforms from the basic elastodynamic equations and assumed earth structures. Here, we use a technique known as the "reflectivity method" which can calculate accurate theoretical seismograms with very few restrictive mathematical approximations (Kind, 1978). The most restrictive approximation is the requirement that earth models are vertically stratified and laterally homogeneous. This is a reasonable assumption for the present problem, but even for lateral heterogeneity, auxiliary calculational techniques (not discussed here) can help estimate corrections to the theoretical reflectivity method waveforms. Figure 5 is a synthetic seismic-record section for a crustal model of the Rio Grande rift derived from analysis of the complete 350-km-long DICE THROW profile (Olsen and others, 1979). Assumed variation of P-velocity with depth is shown in Figure 5b. This P-velocity model matches all the DICE THROW travel time data. Relative amplitudes of phases within a seismogram and the variation of phase amplitudes with distance are also functions of S-wave velocities (S-velocities not plotted in Figure 5). In particular, Olsen and others (1979) showed that in order to explain abnormally large amplitudes of P x P for ranges between 40 and 100 km (P x P emphasized by light shading in fig. 5a), S-wave velocity at the top of the lower crust has to be smaller than the nominal value given by the standard V_p/V, ratio of "0= 1.73 (equivalent to a Poisson's ratio of 0.25) which pertains to crustal rock under normal conditions.

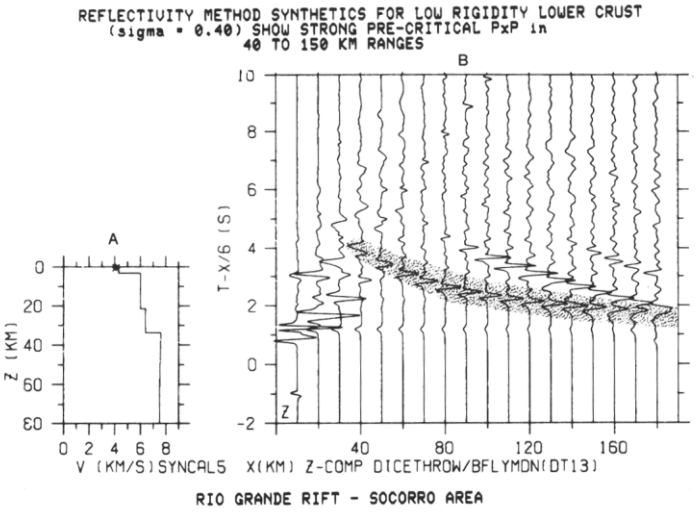

Figure 5. (a) Vertical component synthetic-seismogram record section calculated by the modified reflectivity method. Plot is the same format as observations in Figure 3 and shows strong P×P phases produced by assumed low-rigidity material properties at midcrustal depth. True relative amplitudes are obtined by dividing each trace by a factor proportional to distance to the 3/2 power. (b) Assumed P-velocity crustal model.

Poisson's ratio is a measure of the V_p/V, ratio and is a convenient parameter indicating the degree of rigidity of rocks. Poisson's ratio for crustal rock near the surface is usually about 0.25 (0.03). Higher Poisson's ratio indicates lowered rigidity (i.e., lowered V_p/V_s); Poisson's ratio = 0.5 indicates a fluid of no rigidity and $V_s = 0$.

Synthetic seismograms illustrated in Figure 5 were calculated with a Poisson's ratio of 0.4 for the lower crust (equivalent to V, =- V,/ 1/13= 2.6 km/s rather than the nominal V, = 3.7 km/s, a 30 percent reduction, and represent a slight overestimate of the observed P x P amplitudes in Figure 3). Synthetics calculated with nominal V,— 3.7 km/s show very weak P x P; synthetics with V, = 3.1 km/s (16 percent reduction, Poisson's ration = 0.35) give reasonable matches to P x P observations shown in Figures 3 and 4. Thus, synthetic modeling of refraction observations shows that the wide-angle P x P reflection phases must be accounted for mainly by a decrease in S-velocity; decrease of V, alone is relatively ineffective in enhancing wide-angle P x P.

Although the main characteristics of various reflections from the MCMB can be accounted for by synthetic modeling, a clearer insight into how various physical properties of the MCMB affect different aspects of the reflections can be gained by isolating that part of the synthetic-seismogram program that calculates the ratio of incident seismic energy to reflected seismic energy only for waves reflected from the midcrustal interface. We further simplify the analysis to a plane-wave approximation. We show the results in the form of three-dimensional plots of reflectivity (ratio of reflected-to-incident amplitudes) as functons of frequency and angle of incidence (0° incidence is vertical, 90° is grazing; for reflection, angles of incidence and reflection are equal).

Figure 6 is a three-dimensional plot of P x P reflection coefficients for a simple case of two homogeneous half-spaces separated by a sharp, planar interface. P-velocity is 6.0 km/s in the upper region and 6.4 km/s in the lower, which is the DICE THROW crustal model for the Rio Grande rift. In Figure 6a, the ratio of V, to V, equals the nominal value of "0 on both sides of the discontinuity; whereas, for Figure 6b, V_p/V,= V6 only for the lower region, which is the case for which the synthetics of Figure 5 are calculated.

Three facts should be kept in mind when interpreting these reflection coefficient diagrams as well as those of Figures 7 and 8. First, there is no frequency dependence for a planar first-order velocity discontinuity, so the results given in Figure 6 apply to the higher frequencies (10 to 35 Hz) of the COCORP and microearthquake observations as well as lower frequencies (1 to 4 Hz) of refraction profiles. Only the 0 to 4 Hz frequency range is plotted in Figure 6. Secondly, for angles of incidence greater (i.e., more grazing) than about 70°, the reflection coefficient is unity, which means incident grazing P-wave energy is totally reflected. The distance or angle of incidence beyond which total or near total reflection occurs is defined as the critical distance or angle. Thirdly, typical angles of incidence for pre-critical, wide-angle P x P observations lie between about 30° and 60° (light shading in fig. 6). On the

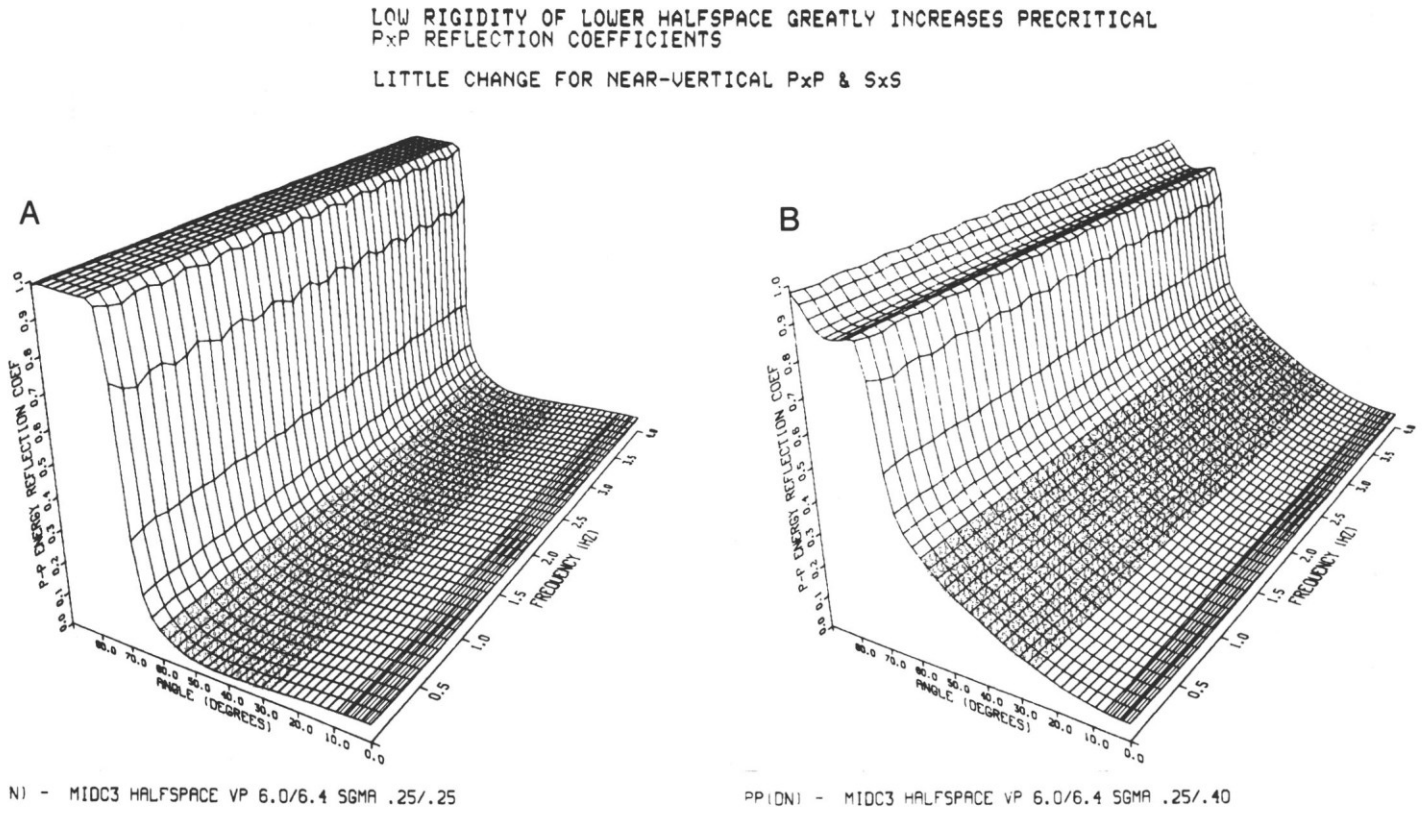

Figure 6. Plots of reflection coefficients (square root of energy normalization) as function of incidence angle and signal frequency for P-to-P reflections from a simple velocity discontinuity between two homogeneous isotropic half spaces. Both plots pertain to P-velocities of 6.0 km/s in the upper layer and 6.4 km/s in the lower. At left, the V_p/V_s ratio remains constant ($= 1.73$) across the interface. At right, the V_p/V_s ratio changes from 1.73 (upper) to 2.45 (lower). Range of incidence angles pertinent to wide-angle refraction profiling lie between 30° and 60°. Vertical incidence is 0°.

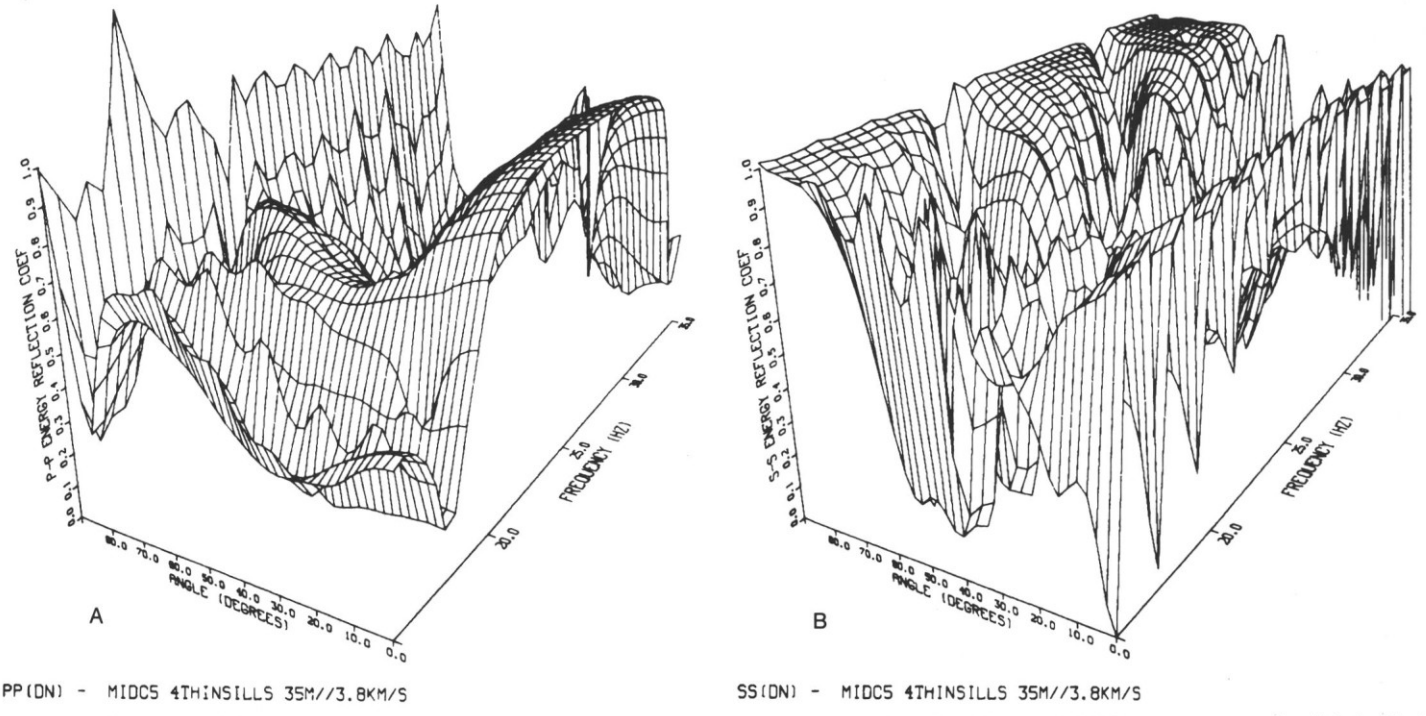

Figure 7. At left is the P-P reflection for stack of four 35-m-thick fluid sills separated by 60-m-thick layers of 6.0 km/s country rock, all imbedded in 6.0 km/s material. Complex angular and frequency dependence is caused by constructive and destructive interference in the thin layers. At right is the S-S reflection coefficient for the same sill model.

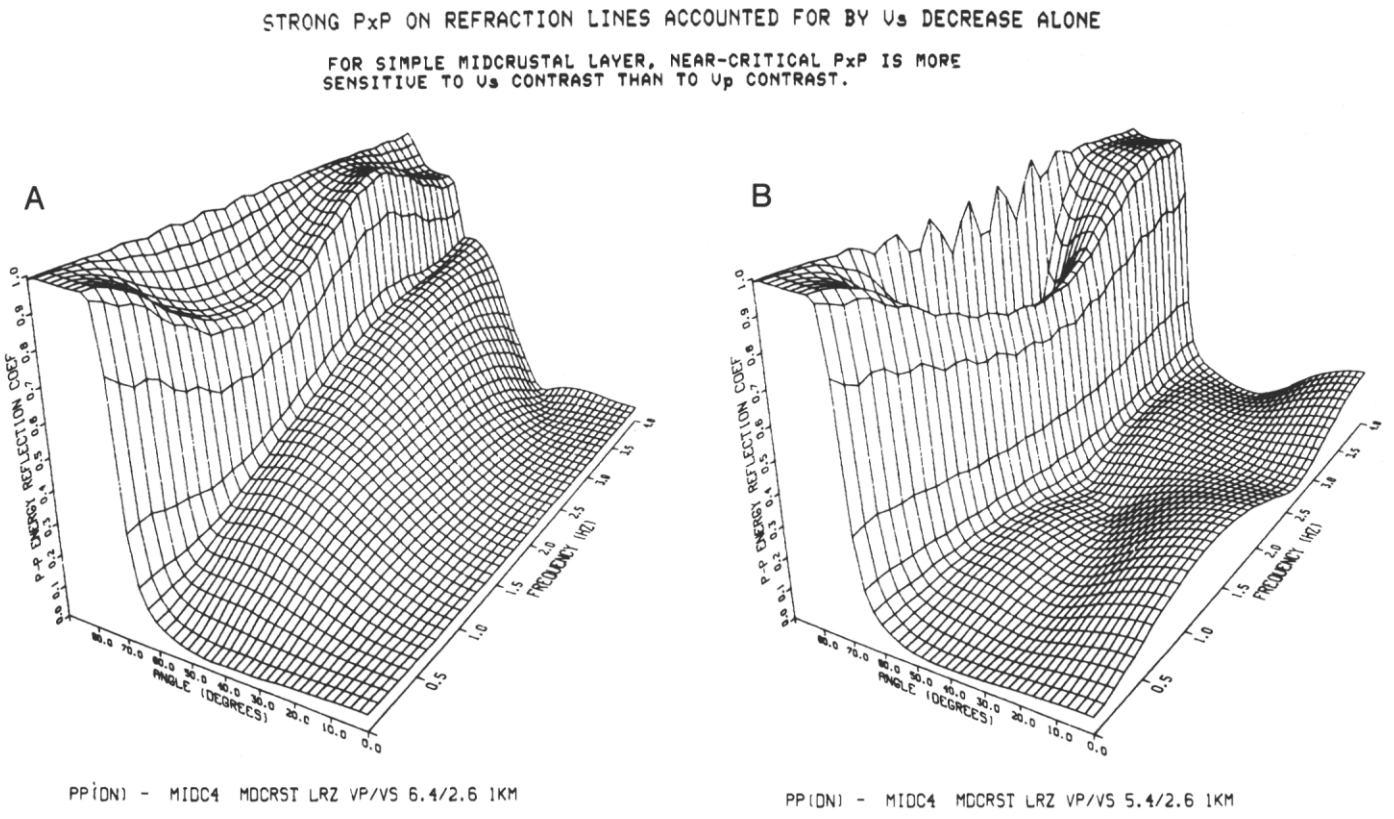

Figure 8. P-P reflection coefficient for 1-km-thick, low-rigidity layer separating 6.0/6.4 km/s upper and lower crust. $V_s = 2.6$ km/s for both plots. At left there is no reduction in the 6.4 km/s P-velocity of the low-rigidity layer. At right there is reduction of P-velocity to 5.4 km/s.

other hand, both COCORP P x P and microearthquake S x S surveys strongly emphasize near-vertical angles (0° to 10°; darker shading in fig. 6).

In Figure 6a (no rigidity or V_p/V_s contrast), note that P x P reflections from the 6.0- to 6.4-km/s P-discontinuity are weak (coefficient less than 0.1) for both vertical and wide-angle profiling. On the other hand, when the material below the interface has low rigidity as in Figure 6b, wide-angle P x P reflections become substantially stronger while near-vertical reflections remain unchanged. The S x S reflection coefficients (not shown) for these two interface discontinuity examples look very similar to P x P in Figure 6. The apparent discrepancy between MCMB areas mapped by refraction and by vertical profiling techniques is thus readily explainable in terms of elementary properties of reflection coefficients for simple differences in material properties on each side of the interface.

As noted above, Brocher's (1981) analysis of COCORP lines suggests that rapid and complicated variations in strong, near-vertical reflections are caused by interference effects in an alternating stack of thin partial melt sills and country rock. Figure 7 is a plot of P x P and S x S coefficients for the case of four 35-m-thick fluid ($V_s = 0$) sills having (low) $V_p = 3.8$ km/s, each separated by 60 m of 6.0 km/s country rock. This entire 0.32-km-thick structure is sandwiched between 6.0 km/s half spaces and is the model considered in Figure 9 of Brocher (1981).

Note that the frequency range of the Figure 7 plots is confined to a high-frequency interval (15 to 35 Hz) pertinent to COCORP/microearthquake observations. Coefficients shown in Figure 7 are complicated and illustrate rapid frequency and angular variations characteristic of interference effects. Since constructive as well as destructive interference occurs, energy in certain angle and frequency ranges can propagate in a "trapped" mode laterally through the transition zone and later emerge greatly reinforced, leading to apparent reflection coefficients greater than unity ("beaming"). The zero-angle P x P curve of Figure 7a closely reproduces the large reflection peak near 25 Hz calculated by Brocher (1981). Brocher argues that even this four-layer sill model is too simple to reproduce all the rapid frequency and spatial variations of reflections observed on COCORP line 1. The large peak near 25 Hz does, however, indicate the central part of the MCMB is composed of complexly layered, anomalous material having a total thickness less than 1 km. Extension of the P x P reflection coefficient plot to lower frequencies (1 to 4 Hz) pertinent to refraction observations (not shown here) shows both vertical and wide-angle coefficients trending toward low values near 0.1, especially if the low P-velocity sills are not completely fluid. Low-frequency coefficients are not as complicated as high- frequency ones, because they pertain to wavelengths considerably longer than sill thicknesses. Synthetic seismograms calculated for refraction profiles similarly do not show extreme P x P amplitude and waveform variations, because of lack of resolution of the dominant longer wavelengths; but rather they indicate average properties of the material over approximately 1-km total thickness.

Figure 7b illustrates the S x S reflectivity function at high frequencies characteristic of microearthquake observations. Although reflection efficiency undergoes rapid cyclic (interference) variations (the details of which are sensitive to assumed S-velocity), in general, the averaged S x S coefficient for near-vertical angles exceeds 0.7, as noted previously by Sanford and others (1977). The averaged reflectivity in Figure 7b also shows a decrease for angles near 45° which, when combined with the predominant dip-slip focal mechanism of the Socorro microearthquakes, probably contributes to the decreased effectiveness of the microearthquake method for detecting MCMB reflections with stations more than 30 km from the sources.

The situation with P x P phases observed beneath the eastern flank of the rift during the DICE THROW and BFLY experiments can be

summarized by the coefficient plots of Figure 8. Figure 8a, for the case of a 1-km-thick layer with no V, decrease at the top of the lower crust (i.e., V_s = 6.4 km/s), and a 30 percent decrease in shear velocity (to V_s = 2.6 km/s), indicates strong wide-angle P x P for pre-critical distances/angles, as observed. Vertical P x P would be weak, as also shown in Figure 6a. If, however, the compressional velocity in the midcrustal layer decreases to 5.4 km/s (lower than both the 6.0 km/s upper crust and the 6.4 km/s lower crust), wide-angle P x P would become weak, even though V_s remains low.

DISCUSSION AND CONCLUSIONS

From our modeling studies, we conclude a thin (about 1 km thick) sill-like, midcrustal, low-rigidity zone surrounds the main MCMB, at least on the north and the east where refraction profile data exist. This "aureole" consists of material with S-velocities decreased by up to 20-30 percent from contacting country rock but with little or no P-velocity decrease. This aureole zone may cover an area as large as 2,000 km^2 east of the main MCMB, but this figure is uncertain because of limitations in lengths and azimuths of refraction profiles. Based on absence of observable P x P, it appears the aureole zone (and certainly the main MCMB) terminates north of the latitude of Belen (34.7°N).

In agreement with Brocher's (1981) analysis of high-frequency vertical P x P reflections on COCORP lines, our modeling shows that a strongly laminated midcrustal structure is necessary to explain the observed rapid frequency and lateral variations of the MCMB reflectivity near the center of the rift valley. Substantial decreases in P-velocity (20 to 40 percent) within thin laminae in the MCMB appear to be necessary to account for the magnitude of largest COCORP reflections. Vertical COCORP P x P reflections are not greatly affected by S-velocity anomalies within the MCMB. In contrast, however, the strengths of reflections (S x S and S x P) from microearthquake surveys are principally dependent on subnormal S-wave velocities. Very small or zero S-wave velocities within very thin laminae satisfactorily explain the microearthquake surveys and confirm earlier conclusions that the central region of the MCMB is a partial-melt layer of relatively small total thickness.

The implications of these *in situ* seismic characteristics upon the petrological nature [composition, fraction of partial melt, melt phase geometry, viscosity, seismic attentuation, etc.] of material in the MCMB and its surrounding low-rigidity zone are poorly understood. Mavko (1980) and O'Connell and Budiansky (1977) indicate that the magnitude of decreases in P- and S-wave velocities needed to explain the observations can be easily accounted for by only small percentages of partial melt, especially if the intercrystalline tube geometry for the molten fraction pertains. However, one particular inferred property of the aureole region, that of 20 to 30 percent decrease in S-velocity for no observable decrease in P-velocity, is not apparent from theoretical calculations of elastic moduli for various melt phase geometries by Mavko (1980). Unfortunately, experimental data on this effect at appropriate temperatures and pressures do not seem to be available.

S-wave shadowing observations by Sanford and others (1979) and velocity anomaly analysis by Ward and others (1981) suggest that isolated small "pockets" of magma exist at levels somewhat above the approximately 20 km depth of the MCMB. However, the most striking attribute of the MCMB is its thinness, relatively great lateral extent, and the very small relief of the upper surface. Perhaps as much as 4,000 km^3 of intrusive material is involved in this unusual feature of the Rio Grande rift. Much additional research is needed to understand forces that control and limit magma ascent to midcrustal levels and the mechanism and rates of lateral spreading of the MCMB.

ACKNOWLEDGMENTS

We thank our colleagues at Los Alamos National Laboratory for collaboration and assistance with seismic refraction profiling in the Rio Grande rift. We particularly thank C. Newton for the data of Figure 4. F. Homuth, T. Handel, B. Hoffers, H. Kepler, J. Wolff, and G. Elbring participated in field work and analysis. We are indebted to E. Rinehart of Air Force Weapons Lab (AFWL) and L. Jacksha of USGS for sharing results of their BUTTERFLY MAIDEN data prior to publication. B. Stump of AFWL played a key role in coordinating BUTTERFLY MAIDEN schedules and countdown activities with Los Alamos field parties. The cooperation and efficiency of P. O'Rourke in preparing the manuscript was invaluable. This research was supported by the U.S. Department of Energy.

REFERENCES

Brocher, T. M., 1981, Geometry and physical properties of the Socorro, New Mexico, magma bodies: Journal of Geophysical Research, v. 86, p. 9420-9432.

Brown, L. D., Krumhansl, P. A., Chapin, C, E., Sanford, A. R., Cook, F. A., Kaufman, S., Oliver, J. E., and Schilt, F. S., 1979, COCORP seismic reflection studies of the Rio Grande rift, *in* Riecker, R. E., ed., Rio Grande rift: tectonics and magmatism: American Geophysical Union, Washington, D.C., p. 169-184.

Brown, L. D., Chapin, C. E., Sanford, A. R., Kaufman, S., and Oliver, J., 1980, Deep structure of the Rio Grande rift from seismic reflection profiling: Journal of Geophysical Research, v. 85, p. 5173-5189.

O'Connell, R. J. and Budiansky, B., 1977, Viscoelastic properties of fluid saturated cracked solids: Journal of Geophysical Research, v. 82, p.5719-5736.

Oliver, J., 1978, Exploration of the continental basement by seismic reflection profiling: Nature, v. 175, p. 485-488.

Olsen, K. H., Keller, G. R., and Stewart, J. N., 1979, Crustal structure along the Rio Grande rift from seismic refraction profiles, *in* Riecker, R. E., ed., Rio Grande rift: tectonics and magmatism: American Geophysical Union, Washington, D.C., p. 127-144.

Rinehart, E. J., Sanford, A. R., and Ward, R. M., 1979, Geographic extent and shape of an extensive magma body at midcrustal depths in the Rio Grande rift near Socorro, New Mexico, *in* Riecker, R. E., ed., Rio Grande rift: tectonics and magmatism: American Geophysical Union, Washington, D.C., p. 237-252.

Sanford, A. R. and Long, L. T., 1965, Microearthquake crustal reflections, Socorro, New Mexico: Bulletin of the Seismological Society of America, v. 55, p. 579-586.

Sanford, A. R., Alptekin, O. S., and Toppozada, T. R., 1973, Use of reflection phases on microearthquake seismograms to map an unusual discontinuity beneath the Rio Grande rift: Bulletin of the Seismological Society of America, v. 63, p. 2010-2034.

Sanford, A. R., Mott, R. P., Schuleski, P. J., Rinehart, E. J., Caravella, F. J., Ward, R. M., and Wallace, T. C., 1977, Geophysical evidence for a magma body in the crust in the vicinity of Socorro, New Mexico, *in* Heacock, J. G., ed., The Earth's crust: its nature and physical properties, Geophysical Monograph Series 20: American Geophysical Union, Washington, D.C., p. 385-403.

Toppozada, T. R. and Sanford, A. R., 1976, Crustal structure in central New Mexico interpreted from the from the GASBUGGY explosion: Bulletin of the Seismological Society of America, v. 66, p. 877-886.

Ward, R. M., Schlue, J. W., and Sanford, A. R., 1981, Three dimensional velocity anomalies in the upper crust near Socorro, New Mexico: Geophysical Research Letters, v. 8, p. 553-556.

Fold patterns in Precambrian metarhyolite, Manzano Mountains (P. Bauer photo).